Channel waveguide lasers in Nd:LGS crystals

Yingying Ren,[1] Javier R. Vázquez de Aldana,[2] Feng Chen,[1,*] and Huaijin Zhang[3]

[1]*School of Physics, State Key Laboratory of Crystal Materials and Key Laboratory of Particle Physics and Particle Irradiation (Ministry of Education), Shandong University, Jinan 250100, China*
[2]*Laser Microprocessing Group, Universidad de Salamanca, Salamanca 37008, Spain*
[3]*State Key Laboratory of Crystal Materials, Shandong University, Jinan 250100, China*
[*]*drfchen@sdu.edu.cn*

Abstract: Optical channel waveguides have been produced in Nd:LGS laser crystals by using ultrafast laser inscription with a depressed cladding configuration. The cross sectional shape of the cladding waveguides is circular, surrounded by low refractive index tracks, which makes the channel waveguides as three-dimensional tubular structures. Under optical pump of 810 nm light, continuous-wave waveguide lasers at 1068 nm have been achieved at room temperature, with minimum lasing threshold of 54 mW, a maximum slope efficiency of 24% and a maximum output power of 16 mW.

OCIS codes: (230.7380) Waveguides, channeled; (160.3380) Laser materials; (130.3120) Integrated optics devices.

References and links

1. C. Grivas, "Optically pumped planar waveguide lasers, Part I: Fundamentals and fabrication techniques," Prog. Quantum Electron. **35**(6), 159–239 (2011).
2. F. Chen, "Micro-and submicrometric waveguiding structures in optical crystals produced by ion beams for photonic applications," Laser Photon. Rev. **6**(5), 622–640 (2012).
3. E. J. Murphy, *Integrated optical circuits and components: Design and applications,* (Marcel Dekker, 1999).
4. R. R. Gattass and E. Mazur, "Femtosecond laser micromachining in transparent materials," Nat. Photonics **2**(4), 219–225 (2008).
5. K. M. Davis, K. Miura, N. Sugimoto, and K. Hirao, "Writing waveguides in glass with a femtosecond laser," Opt. Lett. **21**(21), 1729–1731 (1996).
6. D. G. Lancaster, S. Gross, H. Ebendorff-Heidepriem, K. Kuan, T. M. Monro, M. Ams, A. Fuerbach, and M. J. Withford, "Fifty percent internal slope efficiency femtosecond direct-written Tm^{3+}:ZBLAN waveguide laser," Opt. Lett. **36**(9), 1587–1589 (2011).
7. J. Siebenmorgen, T. Calmano, K. Petermann, and G. Huber, "Highly efficient Yb:YAG channel waveguide laser written with a femtosecond-laser," Opt. Express **18**(15), 16035–16041 (2010).
8. J. Thomas, M. Heinrich, P. Zeil, V. Hilbert, K. Rademaker, R. Riedel, S. Ringleb, C. Dubs, J.-P. Ruske, S. Nolte, and A. Tünnermann, "Laser direct writing: Enabling monolithic and hybrid integrated solutions on the lithium niobate platform," Phys. Status Solidi A **208**(2), 276–283 (2011).
9. G. A. Torchia, A. Rodenas, A. Benayas, E. Cantelar, L. Roso, and D. Jaque, "Highly efficient laser action in femtosecond-written Nd:yttrium aluminum garnet ceramic waveguides," Appl. Phys. Lett. **92**(11), 111103 (2008).
10. C. Grivas, C. Corbari, G. Brambilla, and P. G. Lagoudakis, "Tunable, continuous-wave Ti:sapphire channel waveguide lasers written by femtosecond and picosecond laser pulses," Opt. Lett. **37**(22), 4630–4632 (2012).
11. Y. Tan, A. Rodenas, F. Chen, R. R. Thomson, A. K. Kar, D. Jaque, and Q. M. Lu, "70% slope efficiency from an ultrafast laser-written Nd:$GdVO_4$ channel waveguide laser," Opt. Express **18**(24), 24994–24999 (2010).
12. J. Burghoff, S. Nolte, and A. Tünnermann, "Origins of waveguiding in femtosecond laser-structured $LiNbO_3$," Appl. Phys., A Mater. Sci. Process. **89**(1), 127–132 (2007).
13. J. Siebenmorgen, K. Petermann, G. Huber, K. Rademaker, S. Nolte, and A. Tunnermann, "Femtosecond laser written stress-induced Nd:$Y_3Al_5O_{12}$ (Nd:YAG) channel waveguide laser," Appl. Phys. B **97**(2), 251–255 (2009).
14. A. Okhrimchuk, V. Mezentsev, A. Shestakov, and I. Bennion, "Low loss depressed cladding waveguide inscribed in YAG:Nd single crystal by femtosecond laser pulses," Opt. Express **20**(4), 3832–3843 (2012).
15. Y. Jia, F. Chen, and J. R. Vazquez de Aldana, "Efficient continuous-wave laser operation at 1064 nm in Nd:YVO_4 cladding waveguides produced by femtosecond laser inscription," Opt. Express **20**(15), 16801–16806 (2012).
16. Y. Jia, J. R. Vazquez de Aldana, C. Romero, Y. Ren, Q. Lu, and F. Chen, "Femtosecond-laser-inscribed BiB_3O_6 nonlinear cladding waveguide for second-harmonic generation," Appl. Phys. Express **5**(7), 072701 (2012).
17. N. Dong, F. Chen, and J. R. Vázquez de Aldana, "Efficient second harmonic generation by birefringent phase matching in femtosecond laser inscribed KTP cladding waveguides," Phys. Status Solidi: RRL **6**(7), 306–308 (2012).

#183612 - $15.00 USD Received 16 Jan 2013; revised 27 Feb 2013; accepted 27 Feb 2013; published 7 Mar 2013

18. H. Fritze and H. L. Tuller, "Langasite for high-temperature bulk acoustic wave applications," Appl. Phys. Lett. **78**(7), 976–978 (2001).
19. Y. Yu, J. Wang, H. Zhang, Z. Wang, H. Yu, and M. Jiang, "Continuous wave and Q-switched laser output of laser-diode-end-pumped disordered Nd:LGS laser," Opt. Lett. **34**(4), 467–469 (2009).
20. Y. Ren, Y. Tan, F. Chen, D. Jaque, H. Zhang, J. Wang, and Q. Lu, "Optical channel waveguides in Nd:LGS laser crystals produced by proton implantation," Opt. Express **18**(15), 16258–16263 (2010).
21. H. Liu, Y. Jia, J. R. Vázquez de Aldana, D. Jaque, and F. Chen, "Femtosecond laser inscribed cladding waveguides in Nd:YAG ceramics: Fabrication, fluorescence imaging and laser performance," Opt. Express **20**(17), 18620–18629 (2012).
22. J. Siebenmorgen, K. Petermann, G. Huber, K. Rademaker, S. Nolte, and A. Tünnermann, "Femtosecond laser written stress-induced Nd:$Y_3Al_5O_{12}$ (Nd:YAG) channel waveguide laser," Appl. Phys. B **97**(2), 251–255 (2009).
23. D. Marcuse, "Loss analysis of single-mode fiber splices," Bell Syst. Tech. J. **56**, 703–718 (1977).

1. Introduction

Optical waveguides, as the basic components of integrated photonics, confine the propagation of light fields in small volumes, reaching relatively high optical intensities inside the structures. Benefiting from this feature, lasing in waveguides could have much reduced thresholds and comparable efficiency with respect to the bulk laser systems [1]. In addition, the small scale of the waveguide laser elements enables the realization of compact circuits for diverse photonic applications [2,3]. Different bulk gain materials have different physical, chemical and optical properties. The construction of various waveguiding structures is always a challenge for those that are with excellent lasing properties but not applicable to some mature and cost-effective fabrication techniques. Ultrafast laser pulses with tens of femtoseconds (fs) can directly modify the properties of the transparent materials in micro or submicrometric scales, inducing refractive index changes in the irradiated volumes [4]. This feature enables femtosecond laser inscription a unique technique to fabricate optical waveguide structures in versatile materials. As of yet, fs laser inscription has been successfully applied to produce waveguides in a number of glasses and a couple of crystals [5–14]. Compared with glasses, the effects on crystal materials of the fs laser pulses are much more complicated. Nevertheless, the well-established model for most crystals is the Type II waveguide, which is constructed typically by two parallel fs-laser induced damage tracks with reduced refractive index [7–13]. Waveguiding core is located in the region between two tracks owing to the positive index changes from the stress induced effect at the surroundings of the tracks, which avoids the degradation of the bulk-related features and shows good thermal stabilities. In Type II structures, the waveguiding along various polarizations may be significantly different, which may limit them, to some extent, from the applications relying on orientation-sensitive effects. More recently, the model of "depressed cladding" structure, which is typically surrounded by a number of low-index fs-laser induced tracks, has shown guidance for orthogonal polarizations [14–17]. Usually the cross sectional shapes of cladding waveguides are circular and the diameters can be very flexible from 30μm to 200μm, fitting the diverse width of light beams from various sources (e.g., fibers) to achieve high coupling efficiency. In addition, better balance of the guidance along any transverse polarizations makes cladding waveguide much more advantageous for either un-polarized light pump of waveguide lasers or polarization-dependent guided-wave frequency conversions [16,17].

The single-crystalline langasite ($La_3Ga_5SiO_{14}$ or LGS) is one of the most attractive piezoelectric crystals for acoustic wave applications [18]. Doped with Nd^{3+} ions, it becomes a disordered crystal and serves as an excellent gain medium for high power solid state laser systems. Combined with the good electrooptic features, it is realizable to obtain Q-switched laser generation by using high quality Nd:LGS crystals under laser diode pumping. Moreover, the large birefringence and broad emission bands are suitable for the self-tunable laser gain operation [19]. Due to the very stable chemical properties of the Nd:LGS crystal, normal methods such as ion in-diffusion or ion exchange are not applicable for the waveguide fabrication. Up to now, only proton implantation was used to produce channel waveguides in Nd:LGS crystal [20]. Unfortunately, the relative high lasing threshold of Nd:LGS crystals and the low coupling efficiency of ion implanted waveguides from the pump beam require higher power pump source. In this work, we report on the fabrication of depressed cladding

#183612 - $15.00 USD Received 16 Jan 2013; revised 27 Feb 2013; accepted 27 Feb 2013; published 7 Mar 2013

waveguides in Nd:LGS with a tubular shape by using fs laser inscription. The continuous wave (cw) waveguide lasers at 1.06μm have been realized along both of the two transverse polarizations. This is, to our best knowledge, the first report on the waveguide lasers in this disordered crystal.

2. Experiments

The *x*-cut Nd:LGS (doped with 1 at.% Nd^{3+} ions) crystals were grown by Czochralski method and were cut to dimensions of 1.4(*x*) × 6(*y*) × 8(*z*) mm^3. The depressed cladding waveguides were produced in the laser facility of the Universidad de Salamanca, as schematized in Fig. 1(a). A Ti:Sapphire laser system (Spitfire, Spectra Physics, USA), delivering 120 fs pulses centered at a wavelength of 795 nm and operating at 1 kHz repetition rate, was used as laser source. The pulse energy was finely controlled with a calibrated neutral density filter and a set of half-wave plates and linear polarizers. The beam was focused through a 40 × microscope objective (N.A. ~0.65) at a depth of 125 μm beneath one of the 8 × 6 mm^2 surfaces, and several tests at different pulse energies and scanning velocities were performed. Optical microscopy (in transmission mode) was used to evaluate the damage tracks produced in the sample and the final irradiation parameters were fixed to 0.84 μJ of pulse energy and 500 μm/s of scanning velocity. Such values were chosen as a compromise between producing a large enough damage in the laser tracks and minimizing the formation of cracks in the sample. The waveguides were then fabricated in the direction parallel to the 8-mm edge: to this end, many different scans were done with the chosen parameters in that direction at different depths of the sample (with 125 μm being the maximum focusing depth), with a lateral separation of 3 μm between adjacent scans and following the desired circular geometry from the bottom to the top. Two tubular-shape structures with diameters of 50 and 120 μm were successfully inscribed inside the sample by this procedure, as one can see from the microscope images of the cross sections (Figs. 1(b) and 1(c)). The material in the core region of the waveguides are expected to be nearly undamaged, as demonstrated in waveguides fabricated by the same procedure in Nd:YAG [21]. Optical microscopy reveals no apparent damage in these areas, showing the potential for good waveguiding and lasing properties. Due to the large stress induced during the writing process, some cracks were produced outside the cladding areas. Nevertheless, these cracks have little or negligible effect on the waveguide properties provided they do not affect the core regions.

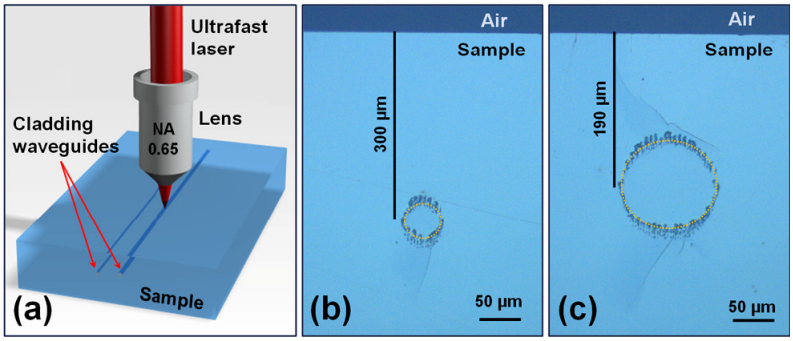

Fig. 1. (a) The schematic of the experimental setup for femtosecond laser inscription, and the microscope image of the cross section for (b) 50 μm and (c) 120 μm diameter cladding structures. The dashed lines indicate the spatial locations of the cladding areas.

The waveguide laser generation experiments were performed by using the end pumping system at room temperature. The pump source used in this work is a Ti:Sapphire continuous wave laser (Coherent MBR 110, USA), which was tuned to emit laser radiation at 810 nm. A half-wave plate was employed to control the polarization of the pump laser beam, so that the waveguide properties in both TE and TM polarization could be investigated. Spherical convex lenses were used to couple the pump laser beam into the waveguides. To achieve high

#183612 - $15.00 USD Received 16 Jan 2013; revised 27 Feb 2013; accepted 27 Feb 2013; published 7 Mar 2013

coupling efficiency between the pump beam mode and the waveguide mode, convex lenses with different focal lengths were utilized. For the 50 μm and 120 μm waveguides, the focal lengths were 50.8 mm and 100 mm, respectively. The Fabry-Perot cavity for the 1.06 μm waveguide laser emission was formed by two dielectric mirrors, which were butt-coupled to the two polished end facets. Thus, the length of the laser cavity was equal to that of the waveguide (around 8 mm). The input mirror has a high reflectivity (>99%) at 1.06 μm and high transmission (98%) at 810 nm, while the output coupler has reflectivity of 95% at 1.06 μm and >99% at 810 nm. The generated waveguide lasers were collected with a 20 × microscope objective lens (N.A. = 0.4). An IR CCD camera and a spectrometer were used to analyze the mode profiles and emission spectra of the generated laser beam. To investigate the losses of two waveguides at the laser emission wavelength, another end coupling system was utilized, in which a cw 1064 nm laser was used as a light source. During this experiment, polarized laser beam at 1064 nm was coupled into and out of the waveguides directly without any mirror. The incident and output powers were detected to calculate the insertion losses of the waveguides. According to insertion loss, the propagation losses can be estimated.

3. Results and discussion

In this work, laser emissions were found in both 50 μm and 120 μm cladding waveguides. Furthermore, laser oscillation was achieved along both of the two transverse polarizations (TE and TM), which has been found to be one of the features of cladding structures. Similar laser emission spectra were obtained from the two different waveguides and the two polarizations. Figure 2, as a representative, gives the spectrum measured from 120 μm waveguide with TM polarization. The central wavelength is 1068 nm, corresponding to the $^4F_{3/2} \rightarrow {}^4I_{11/2}$ transition of Nd^{3+} ions, and the FWHM value of this spectrum is about 2 nm.

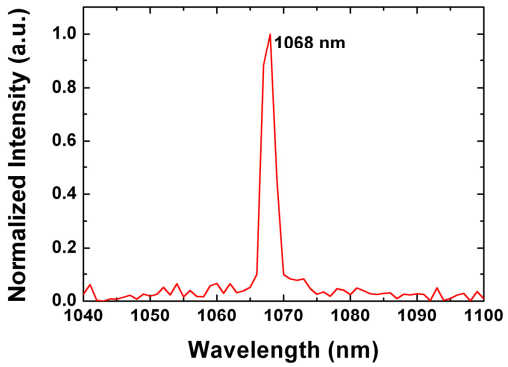

Fig. 2. Normalized spatial intensity distribution of output laser obtained from the 120 μm cladding waveguide when the pumping laser was TM polarized.

Figures 3(a)-3(d) depict the near field intensity distributions of the output waveguide laser generated from 50 μm and 120 μm cladding structures. Figures 3(a) and 3(c) are the modal profiles of 50 μm waveguide, corresponding to TE and TM polarizations respectively, while Figs. 3(b) and 3(d) show the 1068 nm laser mode obtained from 120 μm waveguide, which are also TE and TM polarized. It should be pointed out that the output laser keeps the same polarizing direction with the pump light. As can be seen very clearly from Figs. 3(a)-3(d), the laser modes have quite distinct boundaries, which suggest that the 1068 nm laser are very well confined inside the waveguides during propagation. As expected, both waveguides are multimode at near-infrared wavelength. The 50 μm cladding waveguide, however, has much less mode numbers than the 120 μm one, which imply that single-mode waveguide laser could be achieved when the diameter of the structure is further reduced.

#183612 - $15.00 USD Received 16 Jan 2013; revised 27 Feb 2013; accepted 27 Feb 2013; published 7 Mar 2013

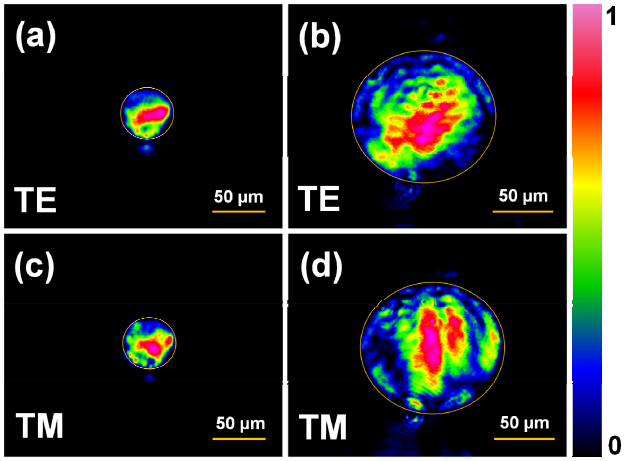

Fig. 3. The output laser mode profiles of the 50 μm ((a) and (c)) and 120 μm ((b) and (d)) cladding waveguides with TE ((a) and (b)) and TM ((c) and (d)) polarization. The yellow circles are the boundaries of the modes. The colors bar in the right show the normalized intensity magnitude of the mode profile.

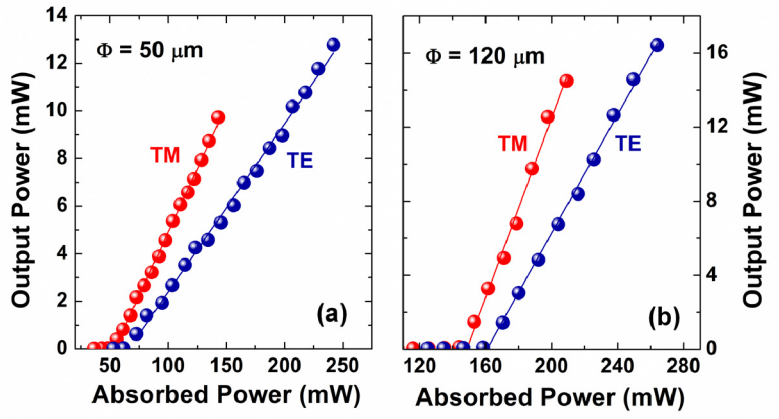

Fig. 4. Dependence between output laser power and absorbed pump power from 50 μm (a) and 120 μm (b) waveguides. The red and blue balls represent the experimental results for TM and TE polarized laser, respectively. The solid lines are linear fit of experiment data.

Figures 4(a) and 4(b) show the experimental results of 1068 nm laser power as a function of the absorbed pump power for the two cladding waveguides. For clarity, the values for lasing threshold, slope efficiency and optical conversion efficiency are summarized in Table 1. As expected, the 50 μm waveguide exhibits lower lasing threshold than that of the larger waveguide. It is obvious that the 50 μm waveguide has smaller effective area, resulting in higher pumping light intensity in the laser cavity. Meanwhile, as mentioned above, the smaller waveguide has less mode number, which means that it has higher coupling efficiency of pump beam into the waveguide. These two factors together contribute to the lower threshold for 50 μm cladding structure. However, the 120 μm waveguide has higher slope efficiency due to its lower propagation loss (see the analysis and calculation results below). Since the two waveguides have their own advantages and disadvantages, they exhibit comparable optical conversion efficiency, from 5% to 7%. Due to the limitation of the input power, the maximum waveguide laser output power was measured to be 16.4 mW when the absorbed power was 264 mW. This result was obtained from TE polarized laser from 120μm waveguide. As one can see from the table, for both of the waveguides, the TM polarized laser

#183612 - $15.00 USD Received 16 Jan 2013; revised 27 Feb 2013; accepted 27 Feb 2013; published 7 Mar 2013

shows better performance than TE polarized one. Compared with the previous work on Nd:LGS bulk laser [19], the most prominent merit for our system is the highly compacted lasing oscillation cavity, which provide us a miniaturized and robust monolithic circuit for near-infrared laser sources. As a matter of fact, no laser performance has been reported from any other Nd:LGS waveguides, indicating that the cladding waveguides fabricated in this work have rather high quality, which, with the combination of promising qualities of Nd:LGS crystal, pave the way for the creation of novel, integrated on-chip Q-switched laser and self-tunable laser devices.

Table 1. Laser performances of Nd:LGS waveguides with diameters of 50 μm and 120 μm

	Lasing threshold (mW)		Max. output power (mW)		Slope efficiency		Optical conversion efficiency	
	TE	TM	TE	TM	TE	TM	TE	TM
50μm	66	54	12.7	9.7	7.1%	10.6%	5.5%	6.8%
120μm	161	148	16.4	14.5	16%	24.2%	6.2%	7%

The change of the refractive index (RI) in the cladding areas was estimated by measuring the maximum incident angle where no change of the transmitted power could be observed [22]. The calculated RI reductions for 120 μm and 50 μm waveguides are approximately 1.4×10^{-3} and 1.2×10^{-3}, corresponding to numerical apertures of around 0.073 and 0.068, respectively. However, the measured RI changes for TE and TM polarizations are slight different (in the order of 2×10^{-4}). Further investigation about the waveguide losses under 1064 nm was performed with an end-coupling system, taking the Fresnel reñection of the end facets (in our case, the value is about 0.1) into account. The insertion losses of the 50 μm and 120 μm waveguides are measured to be (4.5 ± 0.1) dB and (1.3 ± 0.1) dB, respectively, with the difference of 0.2 dB for TE and TM polarizations. Presuming a negligible absorption of 1064 nm wavelength, the propagation loss of the waveguide could be expressed as the difference between the insertion loss and the coupling loss. For 50 μm and 120 μm waveguide, according to Ref [23], the coupling losses caused by the mismatch between the pump beam mode and waveguide mode are calculated to be 0.02 dB and 0.04 dB, respectively. The maximum values of propagation losses of the two waveguides could be therefore estimated to be (5.6 ± 0.1) dB/cm and (1.6 ± 0.1) dB/cm, respectively.

4. Summary

Cladding waveguides with diameters of 50 μm and 120 μm have been fabricated in Nd:LGS laser crystals. The waveguides show well-defined modal profiles and acceptable propagation losses at around 1.06 μm. More importantly, the first ever, to the best of our knowledge, laser oscillation in Nd:LGS waveguide has been realized. The lasing threshold was as low as 54 mW for 50μm-diameter waveguide when the pumping light was TM polarized, whilst the maximum slope efficiency (24.2%) was obtained from 120 μm waveguide. With further optimization of the pump system, one can expect to realize high-quality waveguide laser systems in the fs-laser inscribed Nd:LGS crystals.

Acknowledgments

This work was supported by the National Natural Science Foundation of China (Nos. 11274203 and 11111130200), the Spanish Ministerio de Ciencia e Innovación (Projects CSD2007-00013 and FIS2009-09522), and Junta de Castilla y León (Project SA086A12-2).

#183612 - $15.00 USD Received 16 Jan 2013; revised 27 Feb 2013; accepted 27 Feb 2013; published 7 Mar 2013